A Finite Thin Circular Beam Element for In-Plane Vibration Analysis of Curved Beams

Chang-Boo Kim*, **Jung-Woo Park**, **Sehee Kim**, **Chongdu Cho**
Department of Mechanical Engineering, Inha University,
253, Yonghyun-Dong, Nam-Ku, Incheon 402-751, Korea

In this paper, the stiffness and the mass matrices for the in-plane motion of a thin circular beam element are derived respectively from the strain energy and the kinetic energy by using the natural shape functions of the exact in-plane displacements which are obtained from an integration of the differential equations of a thin circular beam element in static equilibrium. The matrices are formulated in the local polar coordinate system and in the global Cartesian coordinate system with the effects of shear deformation and rotary inertia. Some numerical examples are performed to verify the element formulation and its analysis capability. The comparison of the FEM results with the theoretical ones shows that the element can describe quite efficiently and accurately the in-plane motion of thin circular beams. The stiffness and the mass matrices with respect to the coefficient vector of shape functions are presented in appendix to be utilized directly in applications without any numerical integration for their formulation.

Key Words : Thin Circular Beam, Finite Element, In-plane Motion, Natural Shape Function, Stiffness Matrix, Mass Matrix, Shear Deformation, Rotary Inertia

1. Introduction

The in-plane static or vibration analysis of curved beams is quite complex due to the presence of bending-extension coupling and the effects of shear deformation and rotary inertia. Neglecting these effects may lead to inaccuracies of the analysis especially when the ratio of radial thickness to radius of curvature of a curved beam is not small (thick circular beam), and for vibration problem, natural frequencies of higher modes may be erroneous even though the ratio is very small (thin circular beam).

So far, many papers studying the finite curved beam elements for the in-plane static or vibration analysis of non-straight beams have been reported. The total extent of the works in this field is now too great to be reviewed in detail, but those papers that set the present work in context are briefly summarized in the following.

Davis et al. (1972) presented the shape functions of a curved beam element that are the exact in-plane displacements obtained from an integration of the differential equations of an infinitesimal element in static equilibrium. The stiffness and mass matrices were derived from the force-displacement relations and the kinetic energy equations, respectively. The matrices are formed for the in-plane motion of either a thick curved beam with the effects of shear deformation and rotary inertia or a thin curved beam without those effects. The matrices are formulated in the local straight-beam (Cartesian) coordinate system rather than in the local curvilinear (polar) coordinate system, and thus a transformation of the matrices for the local coordinate system to the one for the common global coordinate system is required before its are assembled even though the radius of curvature for the entire curved beam is

* Corresponding Author,
E-mail : kimcb@inha.ac.kr
TEL : +82-32-860-7383; **FAX** : +82-32-868-1716
Department of Mechanical Engineering, Inha University, 253, Yonghyun-Dong, Nam-Ku, Incheon 402-751, Korea. (Manuscript **Received** December 3, 2004; **Revised** November 1, 2005)

constant.

Ashwell et al.(1971) studied the static application of cylindrical shell element and compared the results with those obtained by using a new element based on simple strain function. A finite element formulation based on natural shape function was also presented but the effect of shear deformation was not considered. Yamada and Ezawa (1977) proposed a straightforward criterion to warrant the displacement functions being used in the finite element approximation of circular arches. The criterion was established by studying the natural shape functions of the exact solutions of the deformed shape of the circular arch element. Meck (1980) developed a finite element solution for a thin curved beam by considering or neglecting the extensional deformation and observed that excellent results could be obtained by using polynomial based displacement functions.

Prathap and Babu (1986) derived a 3-node curved beam element with shear deformation, based on independent iso-parametric interpolations and field consistency principles. This beam element suffered from membrane locking with the increase in the ratio of element length to thickness due to the inconsistency of membrane strain, while the inconsistency in shear strain did not lead shear locking, but degraded the performance of the element and resulted in severe force oscillations. Guimaraes and Heppler (1992) investigated a thin beam element based on trigonometric functions for its ability to recover incremental rigid body motions. They compared the performance of three different models. Choi and Lim (1993) developed two curved beam elements, which are the CSCC and the CSLC elements based on Timoshenko beam theory and curvilinear coordinate system, modified from the conventional strain based shape function element. Lee and Sin (1994) presented the formulation of a 3-node curved beam element based on curvature.

Sabir et al.(1994) developed a strain based curved beam element by using Timoshenko deep beam formulation in the curvilinear coordinate system. A linear variation of bending curvature, and a constant extensional as well as shear strains were chosen. Krishnan and Suresh (1998) obtained the effects of shear deformation on deflection and shear deformation together with rotary inertia on the natural frequencies of curved beams by using a 2-node cubic-linear curved beam element having 4 degrees of freedom per node in local Cartesian coordinate system. Kim and Kang (2003) presented a new highly accurate two-dimensional curved composite beam element based on the Hellinger-Reissner variational principle and classical lamination theory by employing consistent stress parameters corresponding to cubic displacement polynomials with additional nodeless degrees.

In the past four decades, some novel approaches for curved beam elements have been presented, but they are not widely adopted in the practical applications because of their complexity. To avoid the complex formulations by the existing approaches, this paper is concerned about development of a thin circular beam element, i.e. a curved beam element of which radial thickness is very small as compared with radius of curvature and in which the effect of variation in curvature across the cross section is neglected. In this paper, the stiffness matrix and mass matrix for the in-plane motions of a thin circular beam element are derived respectively from the strain energy and the kinetic energy, in different manner of the works by Davis et al.(1972), by using the natural shape functions of the exact in-plane displacements which are obtained from an integration of the differential equations of a thin circular beam element in static equilibrium. The matrices are formulated in the local polar coordinate system with the effects of shear deformation and rotary inertia. If necessary, the matrices can be transformed without difficulties for the global Cartesian coordinate system. Some numerical examples are peformed to verify the element formulation and its analysis capability. The results obtained by using FEM are compared with the theoretical ones to examine the convergence and accuracy of the element. The stiffness and the mass matrices with respect to the coefficient vector of shape functions are presented in appendix to be utilized directly in applications without any numerical integration for their formulation.

2. Thin Circular Beam Element

2.1 In-plane deformations

As shown in Fig. 1, the global Cartesian coordinate system of a circular beam element is $Oxyz$. O is the center of curvature of the element. The cross section perpendicular to the circumferential direction of the element is symmetric with respect to the $\xi-\eta$ plane, and its area is constant. The radius of the centroidal line passing through the center of cross section is a. A half of subtended angle of the element is $\phi=(\theta_2-\theta_1)/2$. The nodes of the element, C_1 and C_2 are on the centroidal line.

When we consider only the in-plane deformations with respect to the $x-y$ plane of a circular beam, the displacement of the center of cross section, C, at an angular position θ has radial component, u_ξ and circumferential component, u_η with respect to a local polar coordinate system, $C\xi\eta\zeta$. The rotation of the cross section at C has axial component, ϕ_ζ which is supposed very small.

The shear strain, γ_ξ, extensional strain, ε_η, and bending curvature, χ_ζ at C of a circular beam are as

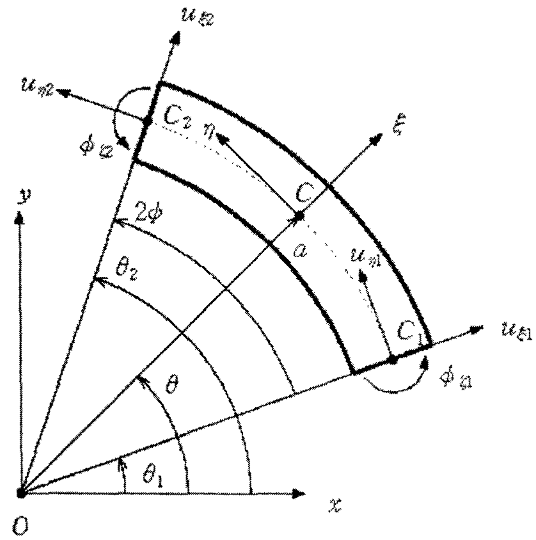

Fig. 1 In-plane displacements of a circular beam

$$\gamma_\xi=\phi_\zeta+\frac{1}{a}(-u_\eta+u_{\xi,\theta}) \tag{1a}$$

$$\varepsilon_\eta=\frac{1}{a}(u_\xi+u_{\eta,\theta}) \tag{1b}$$

$$\chi_\zeta=\frac{1}{a}\phi_{\zeta,\theta} \tag{1c}$$

where $(\ )_{,\theta}$ is a partial differential with respect to circumferential coordinate θ.

When the radial thickness is very small as compared with the radius of centroidal line and the effect of variation in curvature across the cross section is neglected, the beam is called thin.

The internal shear force, N_ξ, extensional force, N_η, and bending moment, M_ζ at C of the thin circular beam are as

$$N_\xi=K_\xi GA\gamma_\xi \tag{2a}$$

$$N_\eta=EA\varepsilon_\eta \tag{2b}$$

$$M_\zeta=EI_\zeta\chi_\zeta \tag{2c}$$

where A, I_ζ, and K_ξ are respectively the area, the area moment of inertia about ζ-axis, and the shear coefficient of the cross section (Cowper, 1966). E is the Young's modulus of the material. G is the shear modulus which is expressed as $G=E/2(1+\nu)$ with the Poisson ratio, ν.

The in-plane strain energy of the thin circular beam element is expressed as

$$V_I=\frac{1}{2}\int_{\theta_1}^{\theta_2}(K_\xi GA\gamma_\xi^2+EA\varepsilon_\eta^2+EI_\zeta\chi_\zeta^2)\,ad\theta \tag{3}$$

The in-plane kinetic energy of the thin circular beam element is expressed as

$$T_I=\frac{1}{2}\int_{\theta_1}^{\theta_2}(\rho A\dot{u}_\xi^2+\rho A\dot{u}_\eta^2+\rho I_\zeta\dot{\phi}_\zeta^2)\,ad\theta \tag{4}$$

where ρ is the density of the material. $(\dot{\ })$ is a partial differential with respect to time, t.

2.2 Shape functions for in-plane deformations

In-plane forces and moments are applied on the cross sections at nodes, C_1 and C_2 of a circular beam element, and the element is in equilibrium.

The internal shear force, extensional force, and bending moment on the cross section at C can be expressed with the internal shear force, $N_{\xi 0}$, extensional force, $N_{\eta 0}$, and bending moment, $M_{\zeta 0}$ on the mid cross section at $\phi=0$ as

$$N_\xi = N_{\xi 0} c\phi + N_{\eta 0} s\phi \tag{5a}$$

$$N_\eta = -N_{\xi 0} s\phi + N_{\eta 0} c\phi \tag{5b}$$

$$M_\zeta = M_{\zeta 0} + aN_{\eta 0} + aN_{\xi 0} s\phi - aN_{\eta 0} c\phi \tag{5c}$$

where $s\phi = \sin\phi$, $c\phi = \cos\phi$

$$\phi = \theta - (\theta_2 + \theta_1)/2 \tag{6}$$

By substituting Eq. (5) into Eq. (2) the shear strain, extensional strain, and bending curvature at C can be expressed with the internal shear force, extensional force, and bending moment on the mid cross section as

$$\gamma_\xi = \alpha_\xi \frac{1}{a}(A_5 c\phi + A_6 s\phi) \tag{7a}$$

$$\varepsilon_\eta = \alpha_\eta \frac{1}{a}(-A_5 s\phi + A_6 c\phi) \tag{7b}$$

$$\chi_\zeta = \frac{1}{a^2}(A_4 + A_5 s\phi - A_6 c\phi) \tag{7c}$$

where

$$A_4 = \left(\frac{a^2}{EI_\zeta}\right)(M_{\xi 0} + aN_{\eta 0}) \tag{8a}$$

$$A_5 = \left(\frac{a^2}{EI_\zeta}\right) aN_{\xi 0} \tag{8b}$$

$$A_6 = \left(\frac{a^2}{EI_\zeta}\right) aN_{\eta 0} \tag{8c}$$

$$\alpha_\xi = \frac{EI_\zeta}{K_\xi GAa^2} \tag{9a}$$

$$\alpha_\eta = \frac{EI_\zeta}{EAa^2} \tag{9b}$$

If $\alpha_\xi = 0$, then the effect of shear deformation is neglected, i.e. $\gamma_\xi = 0$.

The radial displacement, circumferential displacement, and axial rotation of the cross section at C, which are solutions of a system of differential equations obtained by substituting Eq. (7) into Eq. (1), are expressed in terms of ϕ as

$$\begin{aligned} u_\xi = {} & A_2 c\phi + A_3 s\phi - A_4(1 - c\phi) \\ & - A_5(s\phi - e_4 s\phi - e_3\phi c\phi) + A_6 e_3 \phi s\phi \end{aligned} \tag{10a}$$

$$\begin{aligned} u_\eta = {} & A_1 - A_2 s\phi + A_3 c\phi + A_4(\phi - s\phi) \\ & + A_5(1 - c\phi - e_3\phi s\phi) - A_6(e_4 s\phi - e_3\phi c\phi) \end{aligned} \tag{10b}$$

$$\phi_\zeta = \frac{1}{a}\{A_1 + A_2\phi + A_5(1 - c\phi) - A_6 s\phi\} \tag{10c}$$

where A_1/a, A_2, and A_3 are the constants of integration of the system of differential equations, and are respectively the rigid body rotation about the center of curvature in the axial direction, the rigid body displacement of the center of curvature in the radial direction, and the rigid body displacement of the center of curvature in the circumferential direction at the mid cross section.

$$e_3 = \frac{1}{2}(1 + \alpha_\xi + \alpha_\eta) \tag{11a}$$

$$e_4 = \frac{1}{2}(1 + \alpha_\xi - \alpha_\eta) \tag{11b}$$

The static deformations represented by Eq. (10) are used as the shape functions for the in-plane deformations of a thin circular beam element. they are composed of the rigid body modes associated with A_1/a, A_2, and A_3 and the flexible modes associated with A_4, A_5, and A_6. The flexible modes are null at $\phi=0$.

The in-plane displacements and rotations at nodes C_1 and C_2 can be expressed as

$$\{v_I\} = [a_I]\{A\} \tag{12}$$

where

$$\{v_I\} = (u_{\xi 1}\ u_{\eta 1}\ \phi_{\zeta 1}\ u_{\xi 2}\ u_{\eta 2}\ \phi_{\zeta 2})^T \tag{13a}$$

$$\{A\} = (A_1\ A_2\ A_3\ A_4\ A_5\ A_6)^T \tag{13b}$$

$$[a_I] = \begin{bmatrix} 0 & c\phi & -s\phi & -1+c\phi & (1-e_4)s\phi - e_3\phi c\phi & e_3\phi s\phi \\ 1 & s\phi & c\phi & -\phi+s\phi & 1-c\phi-e_3\phi s\phi & e_4 s\phi - e_3\phi c\phi \\ 1/a & 0 & 0 & -\phi/a & (1-c\phi)/a & s\phi/a \\ 0 & c\phi & s\phi & -1+c\phi & -(1-e_4)s\phi + e_3\phi c\phi & e_3\phi s\phi \\ 1 & -s\phi & c\phi & \phi - s\phi & 1-c\phi-e_3\phi s\phi & -e_4 s\phi + e_3\phi c\phi \\ 1/a & 0 & 0 & \phi/a & (1-c\phi)/a & -s\phi/a \end{bmatrix} \tag{13c}$$

The coefficient vector of shape functions, $\{A\}$ then can be expressed in terms of the nodal displacement vector with respect to the local polar coordinate system, $\{v_I\}$, as

$$\{A\}=[a_I]^{-1}\{v_I\} \tag{14}$$

The relationship between the nodal displacement vector with respect to the local polar coordinate system and the nodal displacement vector with respect to the global Cartesian coordinate system, $\{\bar{v}_I\}$, is given by

$$\{v_I\}=[T_I]\{\bar{v}_I\} \tag{15}$$

where

$$\{\bar{v}_I\}=(u_{x1}\ u_{y1}\ \phi_{z1}\ u_{x2}\ u_{y2}\ \phi_{z2})^T \tag{16a}$$

$$[T_I]=\begin{bmatrix} c\theta_1 & s\theta_1 & 0 & 0 & 0 & 0 \\ -s\theta_1 & c\theta_1 & 0 & 0 & 0 & 0 \\ 0 & 0 & 1 & 0 & 0 & 0 \\ 0 & 0 & 0 & c\theta_2 & s\theta_2 & 0 \\ 0 & 0 & 0 & -s\theta_2 & c\theta_2 & 0 \\ 0 & 0 & 0 & 0 & 0 & 1 \end{bmatrix} \tag{16b}$$

2.3 In-plane stiffness matrix

By substituting Eq. (7) into Eq. (3) the in-plane strain energy is expressed in terms of the coefficient vector of shape functions as

$$V_I=\frac{1}{2}\{A\}^T[K_A]\{A\} \tag{17}$$

where $[K_A]$ is the in-plane stiffness matrix with respect to $\{A\}$ of the thin circular beam element. The elements of the symmetric matrix $[K_A]$ is detailed in Appendix.

By substituting Eq. (14) into Eq. (17) the in-plane deformation energy is expressed in terms of the nodal displacement vector with respect to the local polar coordinate system as

$$V_I=\frac{1}{2}\{v_I\}^T[K_I]\{v_I\} \tag{18}$$

where $[K_I]$ is the in-plane stiffness matrix with respect to $\{v_I\}$ of the thin circular beam element as

$$[K_I]=[a_I]^{-T}[K_A][a_I]^{-1} \tag{19}$$

If necessary, the in-plane stiffness matrix for the local polar coordinate system can be transformed for the global Cartesian coordinate system as follows,

$$[\bar{K}_I]=[T_I]^T[K_I][T_I] \tag{20}$$

2.4 In-plane mass matrix

By substituting Eq. (10) into Eq. (4) the in-plane kinetic energy is expressed in terms of the coefficient vector of shape functions as

$$T_I=\frac{1}{2}\{\dot{A}\}^T[M_A]\{\dot{A}\} \tag{21}$$

where $[M_A]$ is the in-plane mass matrix with respect to $\{A\}$ of the thin circular beam element. The elements of the symmetric matrix $\{M_A\}$ is detailed in Appendix.

$$\mu_\zeta=\frac{\rho I_\zeta}{\rho A a^2} \tag{22}$$

If $\mu_\zeta=0$, then the effect of rotary inertia is neglected, i.e. $\rho I_\zeta=0$.

By substituting Eq. (14) into Eq. (21) the in-plane kinetic energy is expressed in terms of the nodal displacement vector with respect to the local polar coordinate system as

$$T_I=\frac{1}{2}\{\dot{v}_I\}^T[M_I]\{\dot{v}_I\} \tag{23}$$

where $[M_I]$ is the in-plane mass matrix with respect to $\{v_I\}$ of the thin circular beam element as

$$[M_I]=[a_I]^{-T}[M_A][a_I]^{-1} \tag{24}$$

If necessary, the in-plane mass matrix for the local polar coordinate system can be transformed for the global Cartesian coordinate system as follows,

$$[\bar{M}_I]=[T_I]^T[M_I][T_I] \tag{25}$$

2.5 In-plane internal forces

By substituting Eq. (7) into Eq. (2) or from Eqs. (5) and (8) the internal shear force, extensional force, and bending moment on the cross section at C can be expressed in terms of the coefficients of shape functions as

$$N_\xi=\left(\frac{EI_\zeta}{a^3}\right)(A_5c\phi+A_6s\phi) \tag{26a}$$

$$N_\eta=\left(\frac{EI_\zeta}{a^3}\right)(-A_5s\phi+A_6c\phi) \tag{26b}$$

$$M_\zeta=\left(\frac{EI_\zeta}{a^2}\right)(A_4+A_5s\phi-A_6c\phi) \tag{26c}$$

3. Numerical Examples

Three problems are selected as numerical examples: 1) linear static analysis for a pinched ring, 2) free vibration analysis for a free ring and 3) free vibration analysis for a circular arc.

Throughout the numerical tests, the values of the material and geometric properties of the rings with rectangular cross section are chosen as follows for the brevity of calculation, unless specified otherwise.

$$E=200\,\text{GPa},\ \nu=0.25,\ \rho=7830\,\text{kg/m}^3,\ a=1\,\text{m}$$
$$A=6\times10^{-3}\,\text{m}^2,\ I_\zeta=5\times10^{-6}\,\text{m}^4,\ K_\xi=0.847$$

3.1 Linear static analysis for a pinched ring

A pinched ring, in which the central loads of magnitude $2P$ are applied at the top and the bottom, is modelled by a quarter ring with the boundary conditions at the two ends as shown in the Fig. 2.

The displacements due to the central load can be obtained analytically from Eqs. (5), (8) and (10) by considering the geometric and natural boundary conditions at the two ends. The radial displacement, $u_{\xi1}$ at the end $\theta=0$ and the radial displacement, $u_{\xi2}$ at the end $\theta=\pi/2$ are

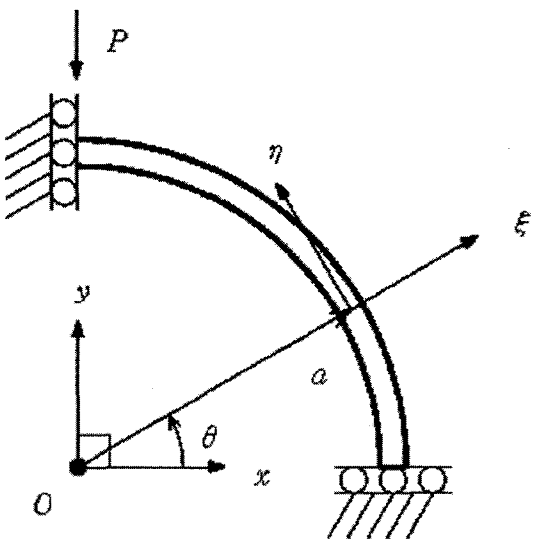

Fig. 2 A quarter ring model of a pinched ring

Table 1 Radial displacements per unit load of a pinched ring

	$\alpha_\xi\neq0$	$\alpha_\xi=0$
$u_{\xi1}/P$ (m/N)	1.3743×10^{-7}	1.3620×10^{-7}
$u_{\xi2}/P$ (m/N)	-1.5136×10^{-7}	-1.4943×10^{-7}

* $\alpha_\xi=0$: neglecting the effect of shear deformation

$$u_{\xi1}=\left(\frac{a^3}{EI_\zeta}\right)\left\{\frac{2}{\pi}-\frac{1}{2}(1-\alpha_\xi+\alpha_\eta)\right\}P \quad (27a)$$

$$u_{\xi2}=\left(\frac{a^3}{EI_\zeta}\right)\left\{\frac{2}{\pi}-\frac{\pi}{4}(1+\alpha_\xi+\alpha_\eta)\right\}P \quad (27b)$$

The above theoretical results are the same as the ones obtained from using Castigliano's theorem by Lee and Sin (1994).

Table 1 summarizes the analytical solutions for the radial displacements per unit load of the pinched ring in the cases of considering or neglecting the effect of shear deformation.

The same results as in Table 1 were obtained by using FEM and modelling the quater ring with only one, two or 16 thin circular beam elements because the shape functions of the element presented in this paper are exact in statics.

3.2 Free vibration analysis for a free ring

The in-plane displacements of a ring which is freely vibrating in a mode having n nodal diameters with a frequency of ω will take the forms

$$u_\xi=(U_{\xi C}\cos n\theta+U_{\xi S}\sin n\theta)\,e^{i\omega t} \quad (28a)$$
$$u_\eta=(U_{\eta C}\cos n\theta+U_{\eta S}\sin n\theta)\,e^{i\omega t} \quad (28b)$$
$$\phi_\zeta=(\Phi_{\zeta C}\cos n\theta+\Phi_{\zeta S}\sin n\theta)\,e^{i\omega t} \quad (28c)$$

Substituting Eq. (28) into Eq. (3) and Eq. (4), integrating around the ring, and applying Lagrange's equations give the following equations

$$[K_{IC}-\omega^2M_{IC}]\{U_{IC}\}=\{0\}\ \text{for}\ n=0 \quad (29a)$$
$$[K_{IA}-\omega^2M_{IA}]\{U_{IA}\}=\{0\}\ \text{for}\ n\geq1 \quad (29b)$$

where

$$U_{IA}=\begin{Bmatrix}U_{IC}\\U_{IS}\end{Bmatrix} \quad (30a)$$

$$M_{IA}=\begin{bmatrix}M_{IC}&0\\0&M_{IC}\end{bmatrix} \quad (30b)$$

Table 2 Convergency of natural frequencies of the in-plane vibration of a ring

Number of nodal diameters	Theory (Hz)	FEM(Hz)/Error(%)			
		16 elements	32 elements	48 elements	64 elements
2	61.891	61.902/0.018	61.893/0.003	61.892/0.001	61.891/0.001
3	173.64	173.90/0.151	173.68/0.025	173.66/0.010	173.65/0.005
4	329.30	331.10/0.548	329.61/0.093	329.42/0.037	329.37/0.020
5	525.35	532.56/1.372	526.60/0.238	525.85/0.095	525.62/0.051
6	758.46	779.44/2.766	762.22/0.495	759.97/0.199	759.28/0.108
0	804.37	834.35/3.727	809.16/0.595	806.26/0.235	805.38/0.126
7	1025.3	1073.6/4.715	1034.5/0.897	1029.0/0.362	1027.3/0.196
1	1137.1	1185.7/4.274	1145.6/0.754	1140.5/0.306	1139.0/0.166

$$K_{IA}=\begin{bmatrix} K_{IC} & -K_{IS} \\ K_{IS} & K_{IC} \end{bmatrix} \tag{30c}$$

$$U_{IC}=(U_{\xi C}\ U_{\eta C}\ \Phi_{\zeta C})^T \tag{30d}$$

$$U_{IS}=(U_{\xi S}\ U_{\eta S}\ \Phi_{\zeta S})^T \tag{30e}$$

$$M_{IC}=\pi\rho Aa\begin{bmatrix} 1 & 0 & 0 \\ 0 & 1 & 0 \\ 0 & 0 & \mu_\zeta a^2 \end{bmatrix} \tag{30f}$$

$$K_{IC}=\frac{\pi EI_\zeta}{a^3}\begin{bmatrix} s_\eta+s_\xi n^2 & 0 & 0 \\ 0 & s_\eta n^2+s_\xi & -s_\xi a \\ 0 & -s_\xi a & a^2n^2+s_\zeta a^2 \end{bmatrix} \tag{30g}$$

$$K_{IS}=\frac{\pi EI_\zeta}{a^3}\begin{bmatrix} 0 & -s_\eta n-s_\zeta n & s_\xi an \\ s_\eta n+s_\xi n & 0 & 0 \\ -s_\xi an & 0 & 0 \end{bmatrix} \tag{30h}$$

$$s_\xi=\frac{K_\xi GAa^2}{EI_\zeta} \tag{31a}$$

$$s_\eta=\frac{EAa^2}{EI_\zeta} \tag{31b}$$

When the effect of shear deformation is neglected, by substitution of Eq. (28) into Eq. (1a) and letting the shear strain to zero, the constraint equations for zero shear strain are obtained as

$$\Phi_{\zeta C}=\frac{1}{a}(U_{\eta C}-nU_{\xi S}) \tag{32a}$$

$$\Phi_{\zeta S}=\frac{1}{a}(U_{\eta S}+nU_{\xi C}) \tag{32b}$$

For $n\geq 1$, there exist two orthogonal modes of which the natural frequencies are same, and the nodal diameters of one mode are rotated by $\pi/2n$ from the nodal diameters of the other.

The above theoretical results are similar as the ones obtained by the previous works (Rao and Sundararajan, 1969; Kirkhope, 1977).

In order to show the convergence of the thin circular beam element presented in this paper, the natural frequencies of the in-plane vibration of a free ring were computed by using FEM, modelling the complete ring with 16, 32, 48, or 64 elements, and considering all the effects of shear deformation and rotary inertia. In Table 2 the lowest eight natural frequencies of the flexible modes computed by using FEM are presented and compared with the theoretical values computed by using Eq. (29). The first one mode for $n=0$ is rotational rigid body mode and the first two modes for $n=1$ are translational rigid body modes.

Table 2 shows that the natural frequencies computed by using FEM converge rapidly from above to the theoretical values with increasing number of elements. The percentage errors in the natural frequencies increase with the number of nodal diameters and the order of frequencies.

In order to know the effects of shear deformation and rotary inertia on the natural frequencies of the in-plane vibration of a free ring, the natural frequencies were computed by using FEM, modelling the complete ring with 80 elements, and considering the effects of shear deformation and rotary inertia. In Table 3 the lowest some natural frequencies of the flexible modes computed by using FEM are presented and compared with the theoretical values computed by using

Table 3 Comparison of natural frequencies of the in-plane vibration of a ring

Number of nodal diameters	$\alpha_\xi \neq 0$, $\mu_\zeta \neq 0$		$\alpha_\xi \neq 0$, $\mu_\zeta = 0$		$\alpha_\xi = 0$, $\mu_\zeta \neq 0$	
	Theory (Hz)	FEM (Hz)/ Error (%)	Theory (Hz)	FEM (Hz)/ Error (%)	Theory (Hz)	FEM (Hz)/ Error (%)
2	61.891	61.891/0.000	61.936	61.937/0.000	62.193	62.193/0.000
3	173.64	173.64/0.003	174.08	174.08/0.003	175.52	175.52/0.000
4	329.30	329.34/0.013	330.97	331.01/0.013	335.56	335.57/0.001
5	525.25	525.52/0.032	529.61	529.79/0.033	540.67	540.68/0.002
6	758.46	758.98/0.067	767.21	767.75/0.070	789.60	789.63/0.004
0	804.37	805.00/0.079	804.37	805.00/0.079	804.37	804.39/0.003
7	1025.3	1026.5/0.123	1040.8	1042.1/0.129	1081.1	1081.2/0.007
1	1137.1	1138.3/0.105	1138.0	1139.2/0.105	1137.1	1137.4/0.029
8	1322.4	1325.1/0.204	1347.3	1350.2/0.217	1413.8	1414.0/0.011
9	1646.6	1651.8/0.316	1683.5	1689.2/0.338	1786.3	1786.6/0.018
2	1798.1	1801.4/0.181	1800.5	1803.8/0.182	1798.1	1800.0/0.106
10	1994.7	2003.9/0.461	2046.3	2056.6/0.499	2196.8	2197.4/0.027
11	2363.9	2379.2/0.645	2432.7	2449.9/0.705	2643.9	2644.9/0.039
3	2543.3	2551.1/0.310	2547.0	2555.0/0.312	2543.3	2549.2/0.235
12	2751.6	2775.5/0.870	2839.8	2867.0/0.959	3125.6	3127.3/0.055
13	3155.3	3191.3/1.139	3264.8	3306.1/1.266	3640.2	3642.9/0.075
4	3316.2	3332.4/0.490	3321.2	3337.7/0.494	3316.2	3329.9/0.415

* $\alpha_\xi=0$: neglecting the effect of shear deformation
* $\mu_\zeta=0$: neglecting the effect of rotary inertia

Eqs. (29) and (32).

Table 3 shows that the natural frequencies computed by using FEM are very accurate as compared with the theoretical values in the all cases. The percentage errors in the natural frequencies increase with the number of nodal diameters and the order of frequencies. Both the effect of shear deformation and the effect of rotary inertia lower the values of natural frequencies of the ring. Neglecting the effect of shear deformation raises the values of natural frequencies more, especially for the higher number of nodal diameters, than neglecting the effect of rotary inertia.

3.3 Free vibration analysis for a circular arc

The circular beam element developed is applied to the analysis of free vibration of a circular arc with subtended angle of 60°. The natural frequencies of the in-plane vibration of the circular arc for hinged-hinged, clamped-clamped, and clamped-hinged boundary conditions were computed by using FEM, modelling the circular arc with 60 elements, and considering all the effects of shear deformation and rotary inertia.

For the comparison of the numerical results by FEM with the ones by PSM (pseudo-spectral method) which are presented in the works of Lee (2003), the values of the material and geometric properties of the circular arc are used as follows.

$$E=200\text{ GPa},\ \nu=0.30,\ \rho=7800\text{ kg/m}^3\ a=1\text{ m}$$
$$A=1.2\times10^{-3}\text{ m}^2,\ I_\zeta=1.2\times10^{-7}\text{ m}^4,\ K_\xi=0.85$$

Table 4 shows that the natural frequencies computed by using FEM are very accurate as compared with those by PSM for all the three boundary conditions. The percentage errors in the natural frequencies increase with the order of vibration mode. The numbers given in table 4 are

Table 4 Dimensionless frequency parameters of the in-plane vibration of a circular arc with subtended angle of 60°

Order of vibration mode	Hinged-hinged boundary condition		Clamped-clamped boundary condition		Clamped-hinged boundary condition	
	PSM*	FEM/ Error (%)	PSM*	FEM/ Error (%)	PSM*	FEM/ Error (%)
1	33.365	33.365/0.001	52.779	52.780/0.001	42.333	42.333/0.000
2	68.985	68.986/0.002	75.973	75.975/0.002	73.727	73.728/0.002
3	101.50	101.50/0.001	117.81	117.81/0.002	107.58	107.58/0.002
4	137.44	137.45/0.004	170.79	170.81/0.011	153.98	153.99/0.008
5	214.73	214.76/0.016	255.14	255.20/0.024	234.65	234.70/0.019

*taken from (Lee, 2003)

the dimensionless frequency parameters λ_i which are defined as

$$\lambda_i = \omega_i \sqrt{\rho A a^4 / E I_\zeta} \tag{33}$$

4. Conclusions

We developed a finite thin circular beam element which describes quite efficiently and accurately the in-plane motions of thin circular beams in which the effects of shear deformation and rotary inertia can be considered partially or totally. The element gives exact results for linear static problems in the case of concentrated loads because the shape functions of the element are exact in statics. The natural frequencies of a free ring, which are obtained by using the element converge rapidly from above to the theoretical values with increasing number of elements. The numerical results by FEM for the natural frequencies of a circular arc under various boundary conditions are in excellent agreement with those by PSM. The stiffness and the mass matrices with respect to the coefficient vector of shape functions are presented in appendix to be utilized directly in applications without any numerical integration for their formulation.

Acknowledgments

This work was supported by INHA UNIVERSITY Research Grant.

References

Ashwell, D. G., Sabir, A. B. and Roberts, T. M., 1971, "Further Studies in the Applications of Curved Finite Elements to Circular Arches," *International Journal of Mechanical Science*, Vol. 13, pp. 507~517.

Choi, J. K. and Lim, J. K., 1993, "Simple Curved Shear Beam Elements," *Communications in Numerical Methods in Engineering*, Vol. 9, pp. 659~669.

Cowper, G. R., 1966, "The Shear Coefficient in Timoshenko's Beam Theory," *Transactions of ASME, Journal of Applied Mechanics*, Vol. 33, pp. 335~340.

Davis, R., Henshell, R. D. and Warburton, G. B., 1972, "Constant Curvature Beam Finite Elements for In-Plane Vibration," *Journal of Sound and Vibration*, Vol. 25, No. 4, pp. 561~576.

Guimaraes, J. E. F. and Heppler, G. R., 1992, "On Trigonometric Basis Functions for C^1 Curved Beam Finite Elements," *Computers & Structures*, Vol. 45, No. 2, pp. 405~413.

Kim, J. G. and Kang, S. W., 2003, "A New and Efficient C^0 Laminated Curved Beam Element," *Transactions of KSME (A)*, Vol. 27, No. 4, pp. 559~566.

Kirkhope, J., 1977, "In-Plane Vibration of a Thick Circular Ring," *Journal of Sound and Vibration*, Vol. 50, No. 2, pp. 219~227.

Krishnan, A. and Suresh, Y. J., 1998, "A Simple Cubic Linear Element for Static and Free

Vibration Analyses of Curved Beams," *Computers & Structures*, Vol. 68, pp. 473~489.

Lee, J. H., 2003, "In-Plane Free Vibration Analysis of Curved Timoshenko Beams by the Pseudospectral Method," *KSME International Journal*, Vol. 17, No. 8, pp. 1156~1163.

Lee, P. G. and Sin, H. C., 1994, "Locking-Free Curved Beam Element Based on Curvature," *International Journal for Numerical Methods in Engineering*, Vol. 37, pp. 989~1007.

Meck, H. R., 1980, "An Accurate Polynomial Displacement Function for Finite Elements," *Computers & Structures*, Vol. 11, pp. 265~269.

Prathap, G. and Babu, C. R., 1986, "An Isoparametric Quadratic Thick Curved Beam Element," *International Journal for Numerical Methods in Engineering*, Vol. 23, pp. 1583~1600.

Sabir, A. B., Djoudi, M. S. and Sfendji, A., 1994, "The Effect of Shear deformation on the Vibration of Circular Arches by the Finite Element Method," *Thin-Walled Structures*, Vol. 18, pp. 47~66.

Rao, S. S. and Sundararajan, V., 1969, "In-Plane Flexural Vibrations of Circular Rings," *Transactions of ASME, Journal of Applied Mechanics*, Vol. 91, pp. 620~625.

Yamada, Y. and Ezawa, Y., 1977, "On Curved Finite Elements for the Analysis of Circular Arches," *International Journal for Numerical Methods in Engineering*, Vol. 11, pp. 1645~1651.

Appendix

The matrix $[K_A]$ is symmetric and any element not defined is zero.

$$K_{Aij}=(EI_\zeta/a^3)\,k_{Aij}$$
$$k_{A44}=2\phi$$
$$k_{A46}=-2s\phi$$
$$k_{A55}=(1+\alpha_\xi+\alpha_\eta)\,\phi-(1-\alpha_\xi+\alpha_\eta)\,s\phi c\phi$$
$$k_{A66}=(1+\alpha_\xi+\alpha_\eta)\,\phi+(1-\alpha_\xi+\alpha_\eta)\,s\phi c\phi$$

The matrix $[M_A]$ is symmetric and any element not defined is zero.

$$M_{Aij}=(\rho Aa)\,m_{Aij}$$
$$m_{A11}=(1+\mu_\zeta)\,2\phi$$
$$m_{A13}=2s\phi$$
$$m_{A15}=-2e_3(s\phi-\phi c\phi)+2(1+\mu_\zeta)(\phi-s\phi)$$
$$m_{A22}=2\phi$$
$$m_{A24}=2(\phi-s\phi)-2(s\phi-\phi c\phi)$$
$$m_{A26}=e_4(\phi-s\phi c\phi)$$
$$m_{A33}=2\phi$$
$$m_{A35}=e_4(\phi-s\phi c\phi)-2(\phi-s\phi)$$
$$m_{A44}=(1+\mu_\zeta)\frac{2}{3}\phi^3+4(\phi-s\phi)-4(s\phi-\phi c\phi)$$
$$m_{A46}=2e_3(\phi^2 s\phi+2\phi c\phi-2s\phi)+e_4(\phi-s\phi c\phi)-2(e_3+e_4+\mu_\zeta)(s\phi-\phi c\phi)$$
$$m_{A55}=e_3^2\frac{2}{3}\phi^3+e_4e_3(s\phi c\phi-\phi c2\phi)-4e_3(s\phi-\phi c\phi)+(1+\mu_\zeta)(3\phi-4s\phi+s\phi c\phi)+(1-e_4)^2(\phi-s\phi c\phi)$$
$$m_{A66}=e_3^2\frac{2}{3}\phi^3-e_4e_3(s\phi c\phi-\phi c2\phi)+(\mu_\zeta+e_4^2)(\phi-s\phi c\phi)$$